DOI: 10.1002/suco.201100020

Diederik Veenendaal*
Jeroen Coenders
Jan Vambersky
Mark West

Design and optimization of fabric-formed beams and trusses: evolutionary algorithms and form-finding

Fabric formwork entails the use of fabrics as the main contact material for a concrete mould. The fabric is either hung or prestressed in a supporting falsework frame. Beams or trusses cast in fabric formwork are inherently non-prismatic and have been shown to offer potential for structurally efficient shapes. The casting of beams or trusses in fabric formwork is a highly non-linear problem due to the interaction of the fluid concrete with the woven, prestressed fabric material. Numerical models need to be developed for the engineering of these elements. To this end, it is demonstrated that it is feasible to integrate manufacturing constraints in an automatic optimization process. This is achieved by creating an automated computational framework that includes fabric form-finding and finite element analysis, which operate within an optimization process that uses principles from biological evolution. The results show structurally efficient and manufacturable beams and demonstrate potential for optimization in general that explicitly includes fabrication considerations.

Keywords: fabric formwork, form-finding, dynamic relaxation, genetic algorithm, differential evolution

1 Introduction

The concept of casting concrete in fabrics has resurfaced at various times and in different forms over the past 100 years [1]. The use of fabric in formworks allows savings on formwork material and results in concrete with unconventional aesthetics. Most applications of fabric formwork tend to have a clear function that is either structural or architectural. Structural examples include shell structures (Fig. 1), foundations, revetments and circular columns, whereas architectural examples include fabric-formed walls and façade panels (Fig. 2), where the fabric is used to create a certain surface texture. Fabric-formed structures that feature architectural expression while serving a main loadbearing purpose do exist, but they are few in number and involve academia for the design. The lack of engineering tools for design and analysis is one reason why the potential of fabric-formed structures is seldom translated into commercial projects.

A comparison can be drawn with the engineering practice of tensile structures. Both often rely on physical modelling during the initial design stages and require form-finding software to determine the geometry and subsequent stresses at later stages. Several aspects of the design process are therefore similar. It would be good if soft-

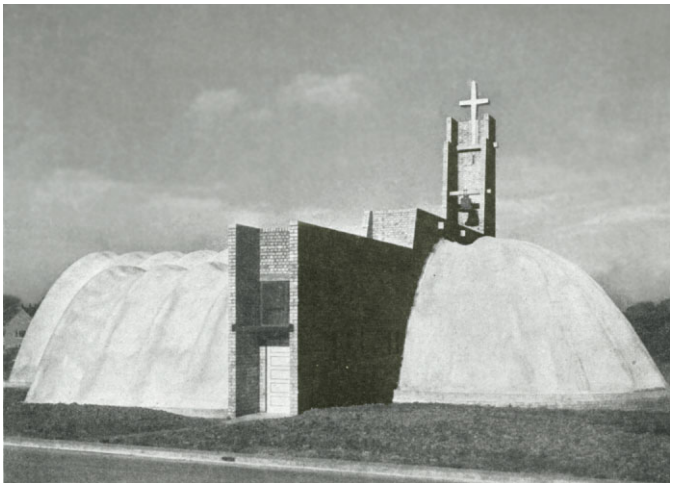

Fig. 1. *James de Waller*, Church of Christ the King and St. Peter, Bristol, 1950 (since demolished), expressive, but entirely shaped by structural considerations; reproduced by permission of the "The Architects' Journal"

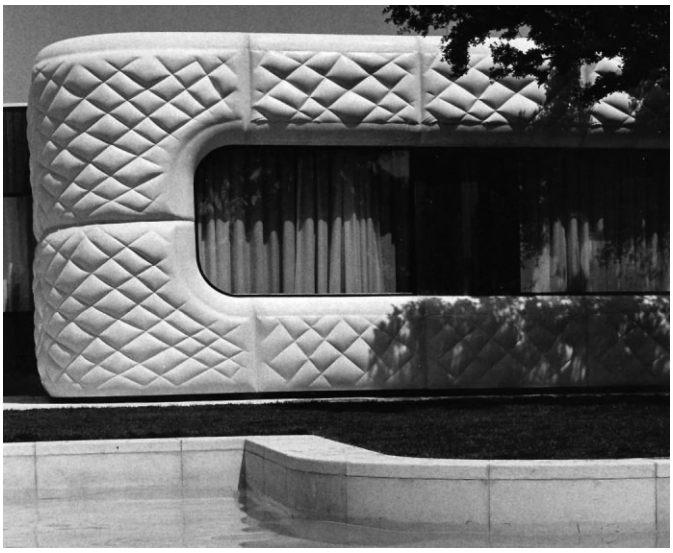

Fig. 2. *Miguel Fisac*, Casa Pascual de Juan en La Moraleja, Madrid, 1975, architectural façade panels, non-loadbearing; reproduced by permission of Fundación Miguel Fisac

* Corresponding author: veenendaal@arch.ethz.ch

Submitted for review: 18 April 2011
Revised: 14 September 2011
Accepted for publication: 14 September 2011

ware tools and modelling were to become available for fabric formwork design as well. They would enable engineers to derive data on the fabric of a fabric formwork such as the prestress, stresses and strains during loading, fabric size and possible cutting patterns. Furthermore, the unconventional concrete geometries that result from fabric formwork have to be understood and analysed as well. General engineering rules of thumb for structural elements often rely on the assumption that the member is prismatic, which may limit how fabric formwork is applied. Overall, a better understanding of the design and engineering of fabric-formed structures is necessary to allow more complex geometries to be realized without input from academia.

2 Scope of the research and approach

The main objective of this research project was to demonstrate the viability of combining an optimization algorithm with manufacturing constraints. The research was carried out at the Faculty of Civil Engineering and Geosciences, Delft University of Technology [14]. Fabric formwork was chosen from current developments in manufacturing methods because it posed interesting and complex constraints. The entire automated computational process that was developed consisted of three main elements: a form-finding algorithm that calculates the shape of the formwork, a structural analysis that evaluates the resulting concrete element and, finally, an optimization algorithm that continually improves on the results.

The interaction with the optimization is as follows: the form-finding is driven by the boundary constraints (e.g. fabric supports and prestressing), its results are evaluated using finite element analysis and these results are then used to determine new "evolved" boundary constraints for the form-finding for a new set of beams.

These three tasks were programmed in a Java framework using dynamic relaxation for form-finding and interfacing with the finite element program ANSYS for structural analysis combined within differential evolution for optimization (Fig. 3).

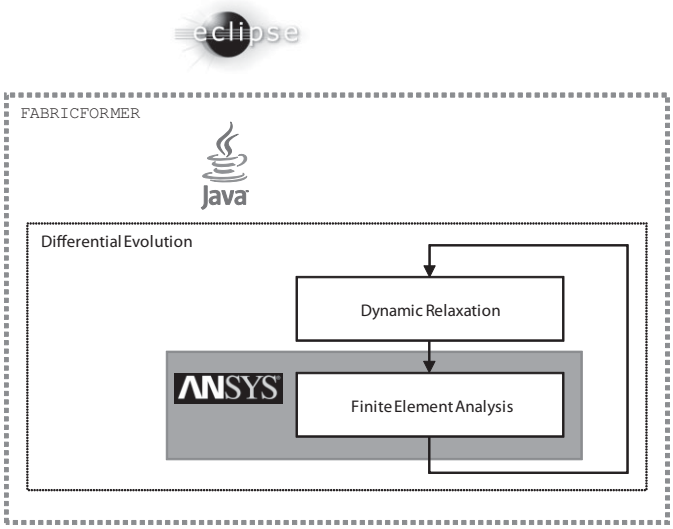

Fig. 3. Simplified diagram of FabricFormer framework

Before discussing each element, an overview is given of existing research on the numerical analysis of fabric formwork and fabric-formed beams to which the software was applied.

3 Existing research

The amount of research on the computational structural analysis of fabric-formed elements is very limited. The only example prior to this research concerns the optimization of fabric-formed panels [2]. A manual iterative procedure was developed to achieve an optimum structural shape for a panel based on its support conditions. The panel was analysed in a finite element program and checked for strength requirements based on the load case. Vrije Universiteit Brussel recently performed studies on the modelling and shaping of fabric formwork. A software program for the design and analysis of tensile structures, EASY, was used [3]. Prototypes made for verification include a non-prismatic column and a hyperboloid-like shell structure. ETH Zurich has used a novel form-finding strategy to calculate the fabric and prestressing required to approximate a given target shape for a fabric-formed shell, applied to a hyperbolic paraboloid [4].

Specific research into fabric-formed beams and trusses has been performed at three other universities. Various methods of manufacturing these elements, such as keel and pinch moulds (Figs. 4 and 5), have been developed at the University of Manitoba in Canada, where the Centre for Architectural and Structural Technology is devoted primarily to research into fabric formwork. Early examples are beams that follow the geometry of the bending moment diagram. Later geometries evolved into trusses as attempts were made to reduce material along the neutral axis of the beam [5]. A related study at the University of Edinburgh investigated a keel mould-type beam [6]. Several consecutive theses at the University of Bath have approached these methods from an engineering point of view [7, 8] and research on the topic remains ongoing. Geometries were optimized for shear and bending resistance, approximated with a fabric formwork and subsequently cast to analyse structural response, material savings and labour costs. The ultimate load capacity was compared with that of a rectangular beam based on the same maximum top width and maximum depth. Results show concrete material savings of 25 % for a keel mould-type beam and 44 % for a beam with a keyhole-shaped section (Fig. 6). The disadvantage of the latter beam is the higher complexity of the formwork required and a corresponding increase in labour costs.

4 Form-finding and analysis

The shape of tensioned membrane structures is not known in advance because it depends on the interaction of boundary conditions, the prestressing of the fabric and the fabric's (non-linear) material properties. A calculation process called form-finding is therefore required. The design and engineering of fabric formworks poses similar considerations and should adhere to the same safety approaches, such as using stress factors instead of load factors (which would change the geometry of the fabric).

Fig. 4. Blackboard diagram of a keel mould (left) and its physical result (right).

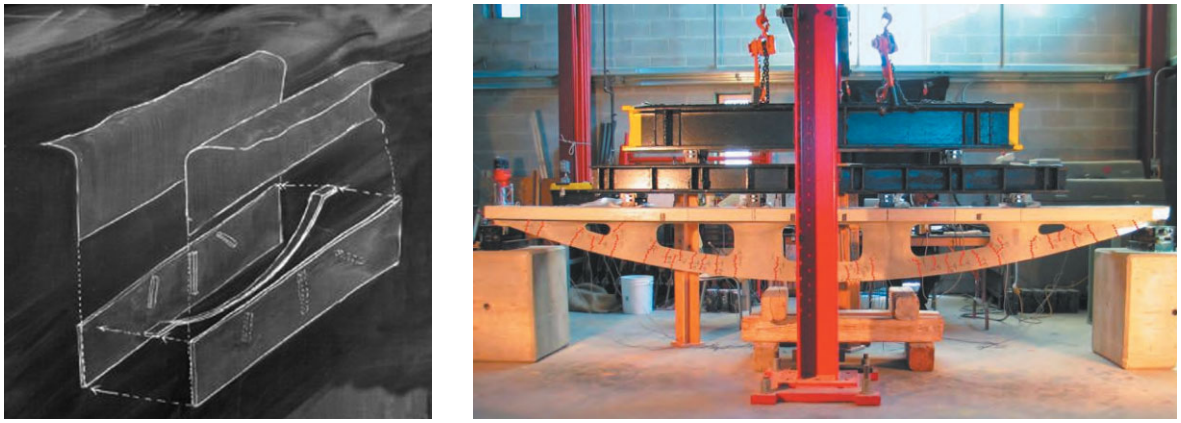

Fig. 5. Blackboard diagram of a pinch mould (left) and its physical result (right)

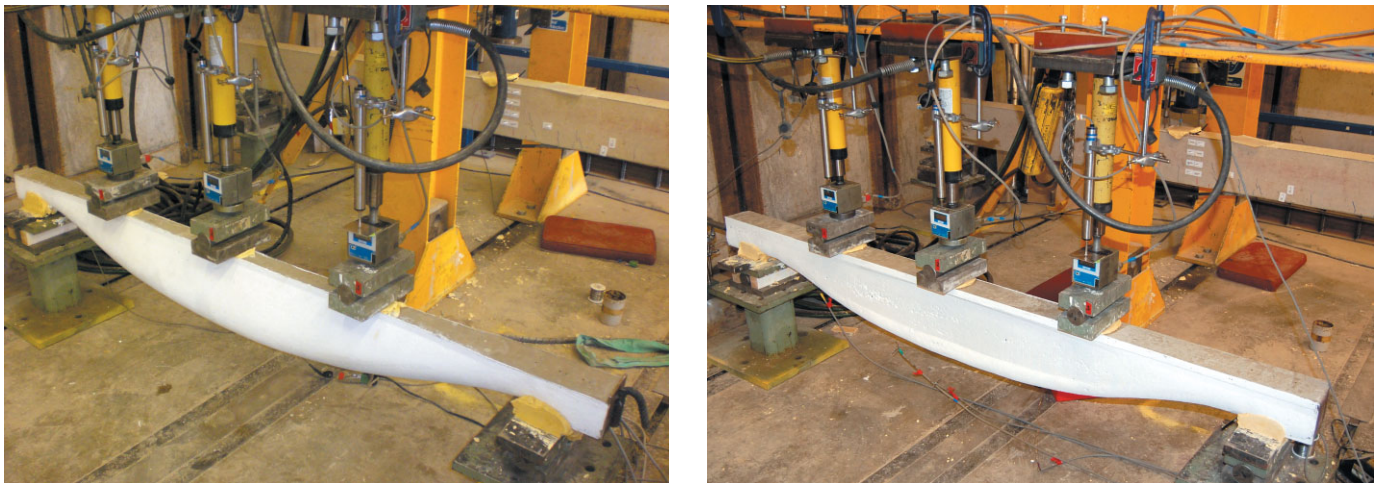

Fig. 6. Keel mould (left) and keyhole-shaped (right) beams undergoing bending tests; reproduced by permission of *Tim Ibell*, University of Bath

However, safety factors and load cases can be less conservative due to the short-term use of fabric formwork. Fabric formwork also introduces the following three complicating factors:

1. The fresh concrete poured into the mould causes a transient load. The stability of the formwork should be considered during casting as well as in the final situation, depending on the concreting operations. The final shape is also influenced by the speed and method of casting due to concrete hardening. As the concrete hardens, the pressures it exerts are no longer entirely hydrostatic because lateral fluid pressures decrease. Furthermore, when permeable fabrics are used, the bleeding of mix water through the formwork membrane further reduces the fluid behaviour of the wet concrete. These effects can be advantageous because the ultimate stress of the fabric will be lower than that in a purely hydrostatic situation, but requires strict limits for the rate of concrete placement to be observed during construction.

2. Some types of fabric formwork introduce rigid elements that push or pull the fabric surface while the fabric is still able to slide in-plane. These elements have been referred to as "pinch points" or "impactos", although in many cases the membrane is fixed to these points. In terms of the modelling of possible sliding, this requires some type of contact analysis or fluid-structure interaction.
3. Several researchers are experimenting with intentional wrinkling and folding of the fabric to create new aesthetics as well as corrugations for buckling resistance. This wrinkling is avoided in typical form-finding procedures that seek to find minimal surfaces or surfaces of mean zero curvature.

For the purposes of this research, the concrete pressure was assumed to be hydrostatic and wrinkling was not considered. Contact analysis is of direct importance to the modelling of more complex fabric-formed beams and was taken into account.

5 Dynamic relaxation

Various form-finding algorithms exist that solve the shape of tensioned membrane structures. The dynamic relaxation algorithm was used in this case [9, 10]. The method of dynamic relaxation is a pseudo-dynamic process in time which is used to solve static problems. In other words, an analogy is drawn between the static solution of a given problem and the equilibrium state of damped structural motion. The algorithm was originally devised for various structural problems and has since been extensively applied to tensile structures as well.

In dynamic relaxation, a discretized shape is set in motion by translating some external load P into an acceleration of the loaded nodes. This results in motion of the nodes, an oscillation (Fig. 7) that will eventually reach static equilibrium due to damping of the movements (Fig. 8). The solution that has been reached is one of minimum potential energy. The dynamic relaxation method was improved by replacing the viscous damping with so-called "kinetic damping" in which the kinetic energy of the whole system is continuously checked for peaks. Whenever such a peak in kinetic energy is detected, all motion is arrested (velocities are set to zero) and the algorithm is restarted at that geometry (Fig. 9). In general, the subsequent peaks decrease in value as equilibrium between the external loads and the internal elastic strains is ultimately achieved.

The following section explains the main formulae and offers some additional information that was found

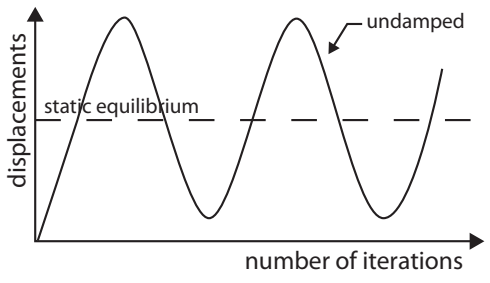

Fig. 7. Undamped oscillations; adapted from *Lewis* [10]

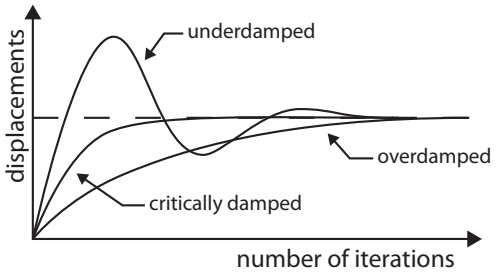

Fig. 8. Viscous damping with damped oscillations; adapted from *Lewis* [10]

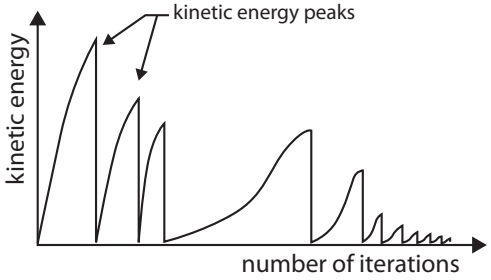

Fig. 9. Kinetic damping with resetting at kinetic energy peaks; adapted from *Lewis* [10]

necessary for the implementation. The authors have noticed that Eqs. (1) and (2) are also known as Leapfrog integration which is closely related to Verlet integration; both are multi-step explicit integration methods for solving dynamic systems. The method equates the residual forces R divided by the lumped mass m (which acts as a stiffness) to nodal accelerations and subsequently determines nodal velocities and positions at each iteration:

$$V_{ij}^{(t+\Delta t/2)} = V_{ij}^{(t-\Delta t/2)} + \Delta t \cdot \frac{R_{ij}^{t}}{m_i} \tag{1}$$

$$x_{ij}^{(t+\Delta t)} = x_{ij}^{t} + \Delta t \cdot V_{ij}^{(t+\Delta t/2)} \tag{2}$$

The lumped nodal masses m are a function of the elastic and geometric stiffnesses of the connecting elements (7). The time increment Δt is no more than a step size for the algorithm. It provides a means of guaranteeing numerical stability and determines the speed at which the algorithm attempts to find a solution. The remaining unknown, the residual, or out-of-balance, force vector R, is the sum of the externally applied loads F and the internal member loads due to tension stiffening for node i in direction j.

$$R_{ij}^{(t+\Delta t)} = F_{ij} + \sum_{i,e=0}^{e=n} \Delta R_{ij,e}^{(t+\Delta t)} \tag{3}$$

where the summation of residual forces consists of:

$$\Delta R_{ij}^{(t+\Delta t)} = \frac{T_e^{(t+\Delta t)}}{L_e^{(t+\Delta t)}} \left(x_k^{(t+\Delta t)} - x_i^{(t+\Delta t)} \right) \tag{4}$$

for each element e. Note that during form-finding, the residual force vectors should converge to zero until a state of equilibrium is reached.

The tension T is determined by the in-plane stiffness, the strain and any initial prestressing.

$$T_e^{(t+\Delta t)} = \frac{EA_e}{L_e^0}\left(L_e^{(t+\Delta t)} - L_e^0\right) + T_e^0 \tag{5}$$

The actual material properties of the elements are not required for form-finding as long as the final stress values are scaled in order to be physically valid. It was decided to calculate the stiffness EA as the product of the linearized modulus of elasticity E_f, the thickness of the fabric t_f and the inradius r of the neighbouring triangle elements, with E_f = 490 N/mm^2 and t_f = 0.76 mm based on a geotextile fabric [2]. In other words, a cable-net analogy was used which is quite common in membrane engineering and simplifies the computations by modelling a continuum as a network of bar elements.

At the end of each iteration, the kinetic energy of the current structure is calculated according to conventional mechanics.

$$E_k^{(t+\Delta t)} = \sum \frac{1}{2} m_i \cdot \left(V_{ij}^{(t+\Delta t/2)}\right)^2 \tag{6}$$

The algorithm converges under the condition that:
- the change in kinetic energy between iterations is sufficiently small, and/or
- the change in displacement between iterations is sufficiently small, or
- a maximum number of iterations is reached, i.e. the solution was not convergent.

The nodal mass m will determine the inertia of each node because it is subjected to forces. As the process of motion is entirely fictitious, these values need not be realistic. It is noted that the precise definition of these fictitious masses is trivial because they only influence the degree of convergence in each iteration, not the final geometry. However, poorly defined masses may lead to divergence. The nodal mass was defined as the sum of the elastic and geometric stiffnesses:

$$m_i = \frac{\Delta t^2}{2} \cdot \sum \left[\frac{EA}{L_0} + \frac{T}{L}\right]_e = \frac{\Delta t^2}{2} \cdot \sum \left[\frac{EA}{L_0} + \frac{EA\varepsilon}{L} + \frac{T^0}{L}\right]_e \tag{7}$$

The inclusion of contact analysis with some of the rigid parts of the mould had to be added to the algorithm. Specific checks were implemented to control fabric that folds along rigid edges of the formwork. Elements that span across an edge retain their correct length and use a temporary third point at the edge as a reference to check this (Fig. 10). In other words, an element is checked if it spans over the edge. If so, the distances to the edge of the two connecting nodes are used as the element length, not the distance between these nodes. Nodes passing over the edge stay within the plane of the fabric – which now folds – and their residual force vector and velocity vector change direction accordingly, using rotation (Fig. 11). The

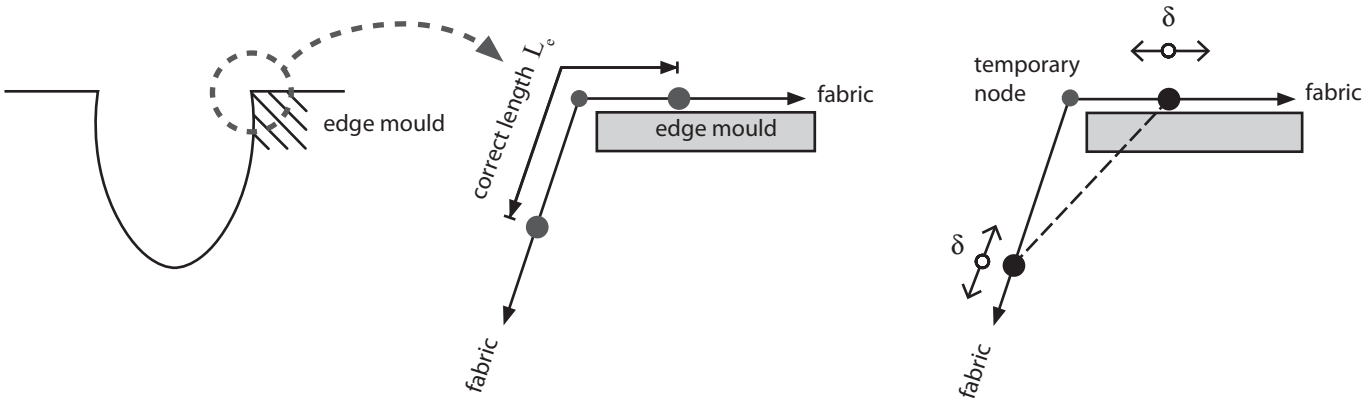

Fig. 10. Diagram of check and correction for elements that fold over the edge of the mould

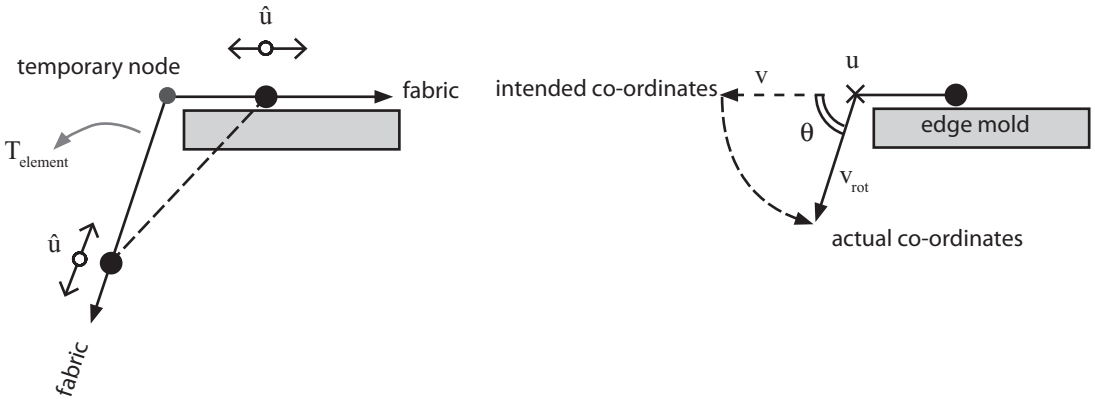

Fig. 11. Diagram of check and corrections for nodes that move over the edge of the mould

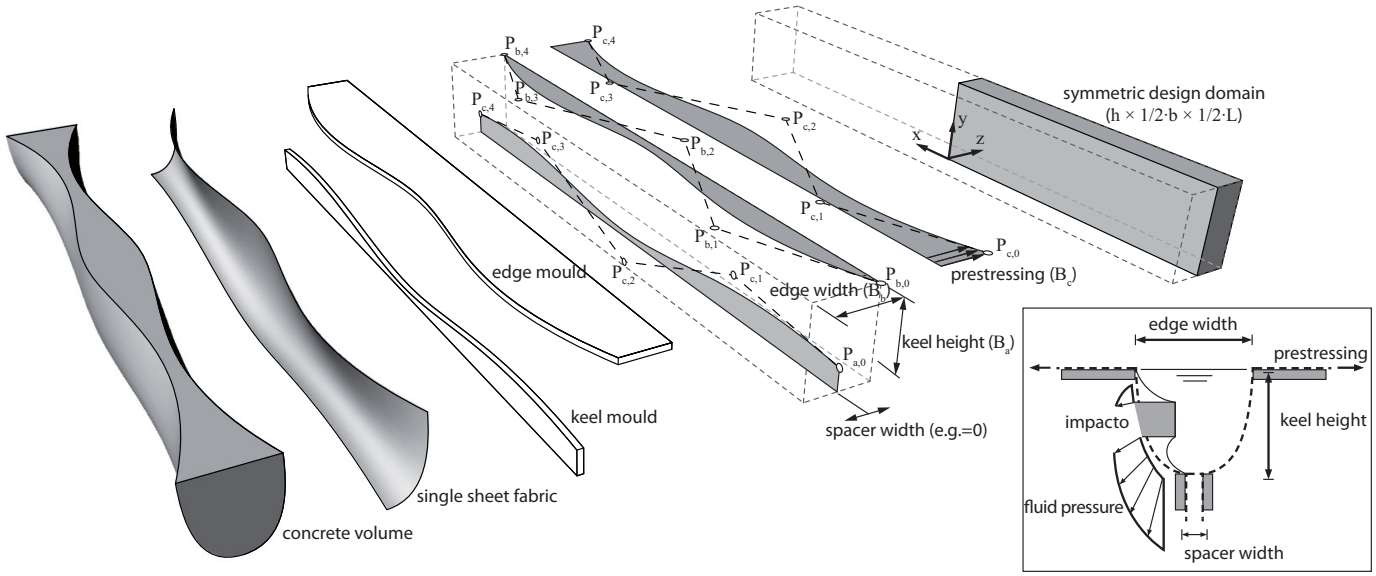

Fig. 12. Design domain, variables and result of a keel mould; inset shows variables for a pinch mould

angle of the adjacent element currently spanning over the edge can be used for this rotation.

The fabric formwork for a beam consists of several elements that, in interaction, determine the ultimate shape of the mould (Fig. 12). The following variables form the target for optimization:

- The prestressing forces along the length of the fabric
- The edge shape along the top
- The keel shape along the bottom
- The width of the spacing strip
- The location and geometry of the pinch points (impactos)

The first three variables – prestress, edge shape and keel shape – were modelled as symmetric, four-degree ($d = 4$) Bézier curves along the length of the span in the x direction (Fig. 12). The y value determines the magnitude of the prestress, the width between the edges and the height of the keel. For a four-degree Bézier curve, the formula is:

$$B(t) = P_0(1-t)^4 + 4P_1(1-t)^3\,t + 6P_2(1-t)^2\,t^2 + \\ + 4P_3(1-t)^1\,t^3 + P_4t^4, t \in [0,1] \qquad (8)$$

where $P_d = \begin{pmatrix} x_d \\ y_d \end{pmatrix}$

and due to symmetry $x_0 = -x_4$, $y_0 = y_4$, $x_1 = -x_3$, $y_1 = y_3$ and due to the fixed, predefined length of the span $x_0 = -1/2\ L$, $x_3 = 0$

This means that only four variables, y_0, x_1, y_1, y_2, remain to be described for each of the three symmetric Bézier curves, resulting in a total of $n = 12$ variables for optimization; these are renamed $x_j = (x_1,\ldots, x_n)$. For the extension to the pinch mould, the spacing strip, a single value, was added later as the thirteenth variable. The pinch points were defined as three quadrangles with four sets of two coordinates and a certain depth to which they impact the fabric. Each quadrangle was mirrored so that there could be six pinch points in total. This resulted in 27 additional variables, $n = 40$ in total, thus increasing the complexity of the model considerably.

6 Structural analysis

Finite element analysis was used within the framework to ensure a fully computational and automated approach. The software application ANSYS was used for the finite element model of the resulting fabric-formed beams. The fabric mesh is first translated into a volume mesh and transferred to ANSYS for evaluation. In this analysis, each beam is subjected to one load case consisting of an evenly distributed load plus self-weight.

A flexible reinforcement strategy for longitudinal reinforcement was implemented and tested, but ultimately not applied in the final results due to computational demands. It was a necessary step, however, in order to demonstrate the feasibility of incorporating non-linear material behaviour in the overall optimization. The non-linear material behaviour of concrete and steel was modelled with bilinear stress–strain curves. The reinforcement required was calculated using an approximation method for non-rectangular cross-sections. This method assumes an alternative stress–strain diagram using a fully plastic stress distribution to avoid complicated calculations. The method assumes two reductions to correct large deviations from more accurately calculated results: the ultimate stress is reduced to $0.95 \cdot f'_c$ and the depth of the compression zone x to $0.80 \cdot x$ (Fig. 13).

The reinforcement is calculated at mid-span and assumes the use of passive prestressing steel because prestressing tendons are ideal for following every possible curvature of the beam. A smeared reinforcement model provided by ANSYS, which averages the local amount of reinforcement per element, is defined by three parameters: the reinforcement ratio and the reinforcement orientation, defined by two angles. These values are calculated for discrete sections along the beam and assumed to have a concrete cover along the bottom. Other than the cover, no check was implemented to evaluate the discrete sizing

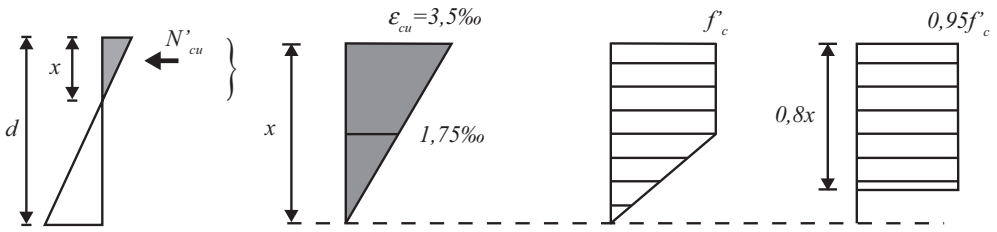

Fig. 13. Approximated stress distribution for non-linear analysis of concrete

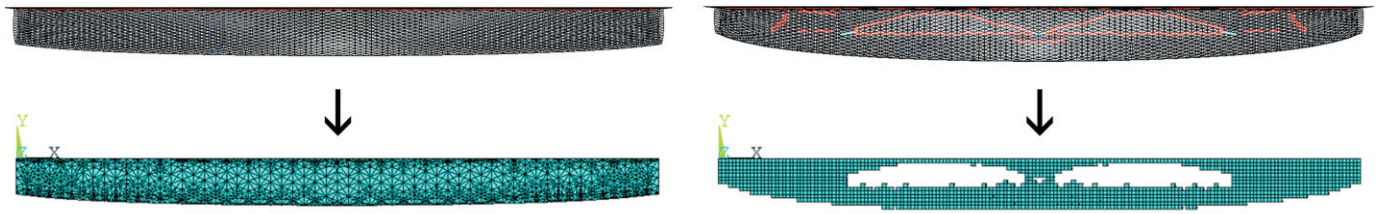

Fig. 14. Change in strategy from ANSYS unstructured meshing (left) to approximated cubic meshing (right)

and positioning of the reinforcement. Note that the resulting reinforcement ratios are very low due to the high strength of prestressing steel and therefore, with a discrete model, cracking behaviour may be a relatively important design issue.

For any calculation in finite elements, some type of element mesh is required. ANSYS provides two kinds of automated unstructured meshing algorithms for meshing complex geometries. Both strategies were tested and applied to the beams that the framework automatically generates and sends to ANSYS for evaluation. Unfortunately, both methods resulted in either a significant percentage of poorly shaped elements despite mesh improvement algorithms, or even failure to mesh the geometry at all. The poorly shaped elements distort the analysis results and therefore the total optimization process. It was decided to approximate the geometry of the fabric formwork using cubic elements of equal size, with the meshing programmed outside of ANSYS (Fig. 14), an approach similar to that used in Bi-Directional Evolutionary Structural Optimization [11]. This results in a less accurate geometry, but keeps the analysis stable and reliable at all times.

7 Optimization problem

The structural analysis is used to evaluate each fabric-formed beam for a single load case of uniformly distributed load plus self-weight. A performance index [11] is calculated as inversely proportional to strain energy x volume. This means that the higher the stiffness of the beam and the lower its volume, the higher the performance will be rated. This induces material optimization while retaining load resistance. As the strain energy is determined by the size of the applied load, the results of the optimization are influenced by the load. The results discussed below give an indication of the sensitivity. For non-linear analysis, the external load is applied incrementally after self-weight while integrating the performance index. This ensures that the entire load history is taken into account while assessing the performance, rather than evaluating the beam for some arbitrary load, thus reducing the sensitivity of the performance index. No integration is necessary for linear analysis, which reduces the computational demand. The optimization including the performance index *PI* is:

$$\min f\left(x_j\right) = \frac{1}{PI} = E_s' \cdot \rho \cdot V = \int_t \int_V \bar{\delta}^T K \bar{\delta} dV dt \cdot \rho \cdot V,$$
$$\text{where } x_j = \left(x_1, \ldots\ldots, x_n\right) \in \mathbb{R} \qquad (9)$$

where
δ displacements
K finite element stiffness matrix
n number of variables determining the shape (Fig. 12)

As explained, the mould is described in part by three Bézier curves – for the shape of the keel, the edge and the magnitude of the prestress – each determined by four coordinates. The bound constraints allow these coordinates to be within one domain distance outside the design domain (e.g. Fig. 12, point $P_{b,2}$) in order to be able to describe a variety of curves within the domain. Additional inequality constraints guarantee that the resulting shape is cut off to stay within the design domain. Indirectly, the form-finding process itself is an equality constraint because it calculates a unique fabric shape in each instance.

The upper and lower bounds $d_{j,U}$ and $d_{j,L}$ of the variables $_{xj}$ are described by the size of the design domain h = 0.8 m, b = 0.3 m, L = 9 m and an ultimate prestress T_U = 40 kN/m [2]. The starting parameters for $x_{j,i,0}$ are randomly generated according to Eq. (10) as discussed below. For the pinch mould, the additional variables are all coordinates within the design domain, constrained to avoid overlap and retaining a quadrangular shape.

8 Evolutionary optimization

The overall process of form-finding, analysis and evaluation has to be guided by a form of optimization towards more optimal geometries. Algorithms already exist that

aim to optimize structural material efficiency, but the results, often described as "organic" or "skeletal", are costly to build. To produce such complex forms, fabric formwork is one option, but the possibilities this method offers come with specific constraints due to the fabric involved. For this reason, the use of a more general purpose optimization algorithm was favoured. Differential evolution is such an algorithm that has the flexibility needed to set up a program that can include the form-finding process for fabrics, and includes non-structural objectives when optimizing for material efficiency, both continuous and discrete variables [12]. The reliability and convergence speed of differential evolution has been shown to be promising compared with other general optimization algorithms [13].

Differential evolution belongs to the category of evolutionary or genetic algorithms. Genetic algorithms use concepts from biological evolution to create a mathematical method of optimization and frequently use the same vocabulary. Evolution is the process by which different kinds of living organisms have developed. In this particular case, a collection of fabric-formed beams can be equated to a generation of living organisms. The information contained in the genes is nothing more than vectors containing variables that describe the fabric formwork. A first set, or generation, of beams is evaluated and those that exhibit superior qualities have a higher likelihood of contributing to the properties of a new generation of beams. Each new beam is generated by combining the properties of parent beams and changing some variables through random mutation. Eventually, after many generations, genetic algorithms find optimal or near optimal solutions. A typical evolutionary algorithm undergoes the following steps, which will be discussed in more detail in this order:
- Initialization
- Selection
- Mutation
- Recombination
- Evaluation
- Termination

The first population can be initialized by any uniform or non-uniform distribution, depending on what is known in advance about the (location of) optima. Nevertheless, a uniform random distribution was chosen to demonstrate the robustness of the entire framework. In this case, each vector component j of beam i is chosen randomly between its feasible lower and upper bounds U and L. The vector components are the variables that determine the shape of the formwork, as shown in Fig. 12.

$$x_{j,i,0} = rand_j(0,1) \cdot \left(d_{j,U} - d_{j,L}\right) + d_{j,L} \tag{10}$$

The size of the population is ideally quite large to cover the range of the solution space, i.e. results in high variance. However, the population size was kept small due to the computational requirements of the entire framework, but this led to poor performance. The final tests were carried out at a compromise of 50 beams per generation.

Selection may take place after evaluating the first population. For each population member, or target vector, three other vectors are selected to calculate a new recombined trial vector against which the target vector is compared. The three other vectors are called the base vector x_{r0} and the random vectors x_{r1} and x_{r2}. Mutually exclusive indices are implemented to ensure that all four vectors are different population members. In differential evolution, the analogy with biological evolution becomes tenuous because in evolutionary terms it could be said that in this case a child (trial) of three parents is compared with one of the parents (target) for selection.

A degree of mutation is introduced at this point to avoid convergence to local optima and to increase variance. This is achieved by adding the vector differences of the random vectors to the base vector. It is from this strategy that differential evolution derives its name. The scale factor F_s gives the weighted difference between the random vectors, which added to the base vector gives the mutant vector $\boldsymbol{v}$ (Eq. (11), Fig. 15):

$$\boldsymbol{v}_{i,g} = \boldsymbol{x}_{r0,g} + F_s \cdot \left(\boldsymbol{x}_{r1,g} - \boldsymbol{x}_{r2,g}\right) \tag{11}$$

where the scale vector for each vector component j is:

$$F_{s,j} = pow\left(rand_j(0,1), q\right) = rand_j(0,1)^q, q = \frac{1}{F} - 1$$

Discrete recombination, better known as crossover, is used to combine two vectors at a crossover point at a vector index C. Vector components 0 to C-1 are taken from one vector and supplemented with components C to D-1 from the other. The crossover factor Cr determines the probability that crossover occurs (Eq. (12), Fig. 16):

$$\boldsymbol{u}_{i,g} = u_{j,i,g} = \begin{cases} v_{j,i,g} & \text{if } \left(rand_j(0,1) \le Cr \text{ or } j = j_{rand}\right) \\ x_{j,i,g} & \text{otherwise} \end{cases} \tag{12}$$

A value of $Cr \approx 0$ produces minimum disruption because few mutant components $v_{i,g}$ are crossed, whereas $Cr \approx 1$ favours a high degree of components from $v_{i,g}$ for the new trial vector $u_{i,g}$. A crossover factor $Cr = 0.2$ is standard, but 0.9–0.95 can be used for limited parameter dependence. Low values proved to be more successful and reliable and

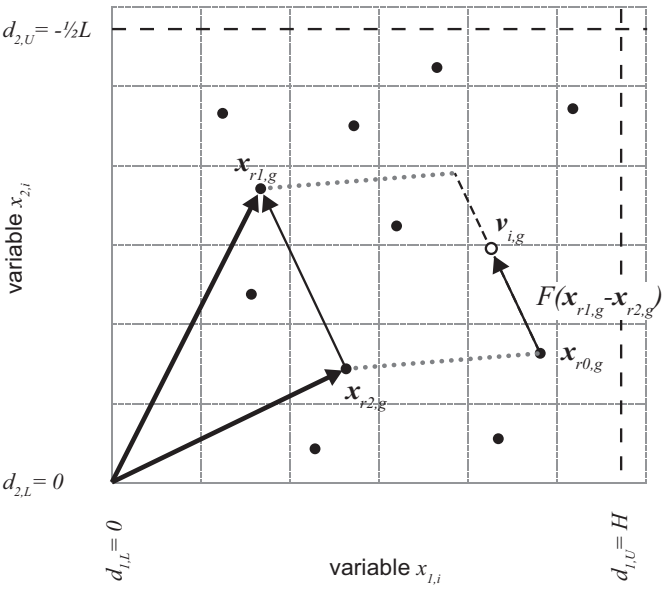

Fig. 15. Projection of vector components x_1 and x_2 for randomly chosen beams r_1 and r_2 in the solution space

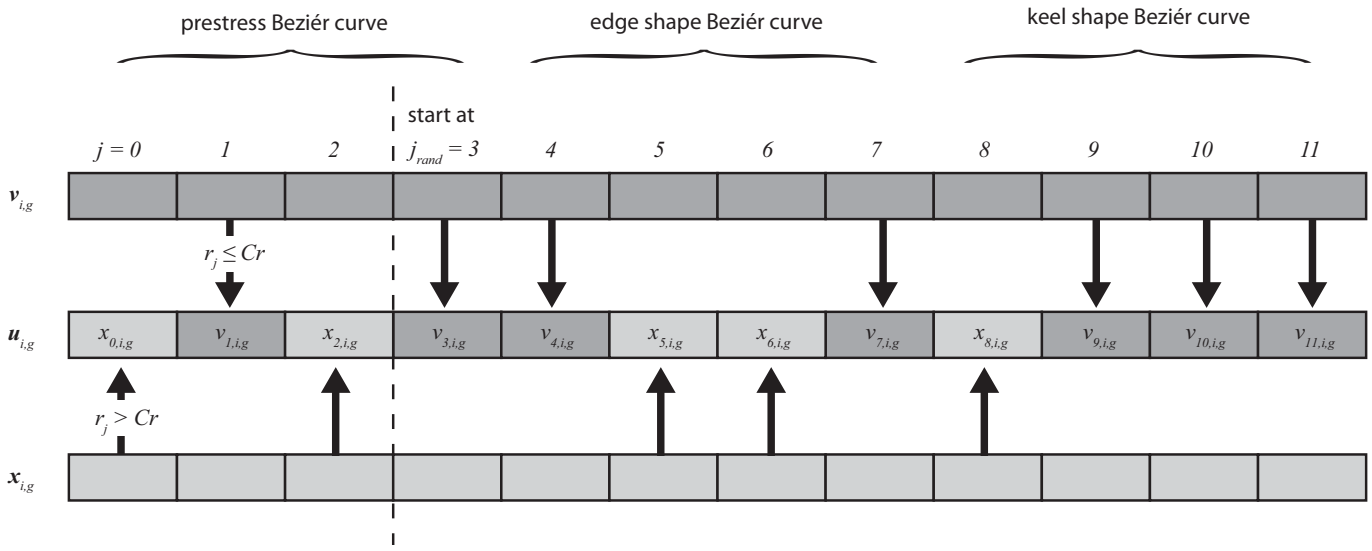

Fig. 16. Recombination from existing and mutant beams $x_{j,i,g}$ and $v_{j,i,g}$ to generate trial beam $u_{j,i,g}$

most tests used $Cr = 2/D$. The last tests for the pinch mould geometries showed a higher dependency on the parameters and therefore used $Cr = 0.9$.

There are various ways of selecting individuals to form a new generation and to reproduce. Differential evolution itself uses one-to-one survivor selection. In this case, each parent (target vector $\boldsymbol{x}$) with index i is compared with the child (trial vector $\boldsymbol{u}$) with the same index (Eq. (13)). The worst-performing vector is discarded. The advantage is that, contrary to some other methods, the best solution so far is always kept and no solution worse than the worst-so-far is ever chosen. On the downside, this means it is possible that a trial vector that is better than most of the current population will be rejected if its target is even better. It became clear that this in fact happens very often in differential evolution. This is not an issue, however, because this merely means that the population will feature a few superior solutions that are the focus of improvement while as a whole will never degrade.

$$\boldsymbol{x}_{i,g+1} = \begin{cases} \boldsymbol{u}_{i,g} \text{ if } PI\left(\boldsymbol{u}_{i,g}\right) \leq PI\left(\boldsymbol{x}_{i,g}\right) \\ \boldsymbol{x}_{i,g} \text{ otherwise} \end{cases} \tag{13}$$

There are various ways of specifying how the differential evolution algorithm should stop, most obviously when improvement in the performance becomes minimal. However, in our case no termination criteria were defined, and progress and termination of the algorithm was carried out manually based on evaluation of continuous output. This was done to avoid creating a black box because practical development of this framework required constant evaluation of the results and convergence behaviour as early as possible, rather than waiting for some specific outcome of arbitrary accuracy.

9 Results

The entire framework, including form-finding, finite element analysis and optimization, is shown in Fig. 17 as a flow chart. During development of the software, results were continuously generated to improve the model. Initial results pertained to the keel mould method, whereas final tests were applied to the pinch mould. One result from each method is shown here for discussion. The first example of the keel mould is shown in Table 1 and Fig. 18. The span of all examples is 9 m. The material models for both fabric and concrete are isotropic, homogenous and linear elastic.

Unfortunately, although the framework proved to be functional, this early result is actually not very optimal. A rectangular beam of equal volume and maximum depth deflects less. This can be expected as the concentration of material shown in Fig. 18 along the neutral axis counteracts the benefits of the curved longitudinal shape. The reason for this result is that the performance index contains two factors that have not been weighted. The reductions in volume weighed heavier than the improvements in stiffness. As the stiffness, calculated as strain energy, is dependent on the load, a higher load would increase the relative importance of stiffness and improve the results. Ideally, the program should use non-linear analysis as discussed because it would allow evaluation of the entire load history up to failure. The strain energy would become a less sensitive value because it would be based on the ultimate load, not an arbitrarily chosen design load. However, due to limits in computational power, it was decided simply to increase the load during later trials. The effect of this was visible because sections tended to become less slender. One later result for the pinch mould is shown in Table 2 and Fig. 19.

This later result is a definite improvement, although the distribution of the impact points is certainly not optimal because we would expect a more optimal result to be comparable with a truss, featuring several openings along the neutral axis instead of merely two large ones. To investigate the potential material-savings of fabric-formed beams, this result was compared with a conventional rectangular beam and a beam with a parabolic, longitudinal profile (Fig. 20).

Some optimum exists between the ratio h_1/h_2 because that would allow the beam to deal with both shear forces and bending moments effectively. Some calcula-

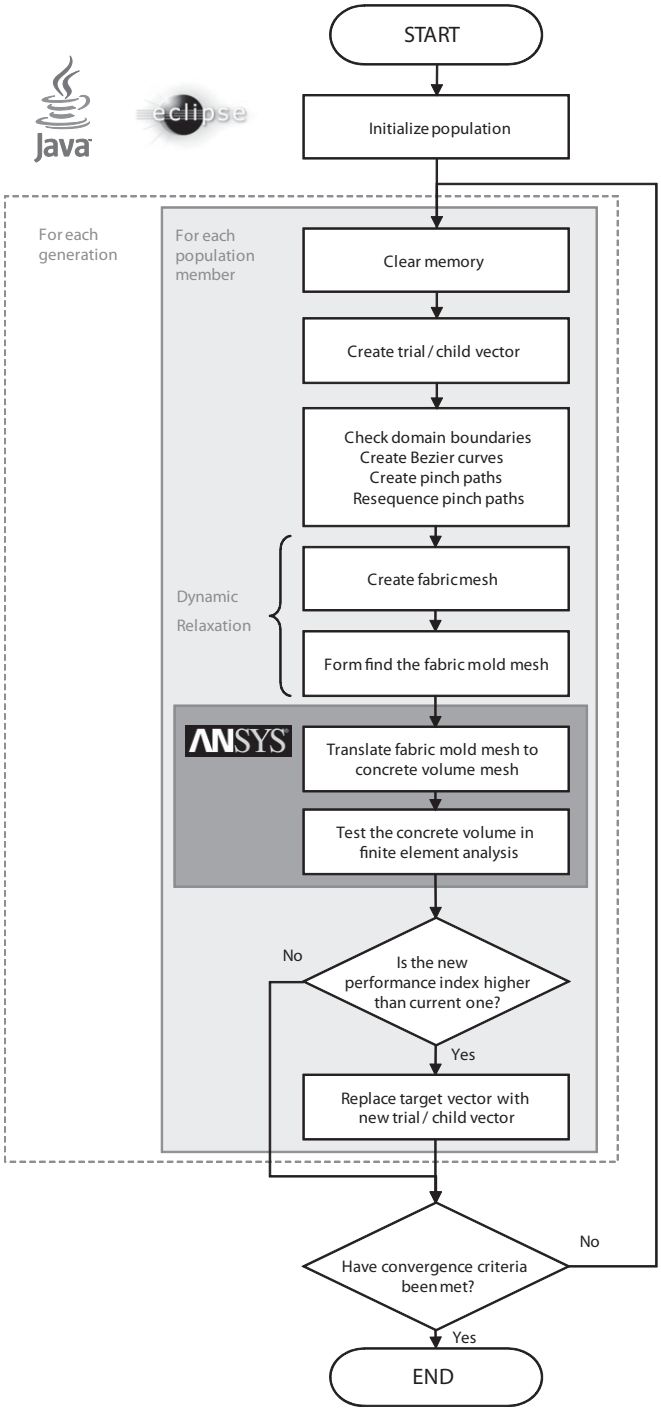

Fig. 17. Flow chart of FabricFormer framework

tions were performed in Maple to calculate the deflection due to distributed loading for different values of h_1/h_2. The calculations are based on energy methods.

The expression for the potential energy for a beam in bending with a uniformly distributed load is:

$$E_{pot} = E_s + E_p = \int \frac{1}{2} M\kappa dx - \int qudx \tag{14}$$

Together with $M = EI\kappa$ and $\kappa(x) = -u_{xx}$ this becomes

$$E_{pot} = \frac{1}{2}\int EI\left(u_{xx}\right)^2 dx - \int qudx \tag{15}$$

Table 1. Results of linear analysis, test No. 33

Stiffness B65	E_c	39394	N/mm^2
Concrete volume	V	0.49	m^3
Mid-span cross-section	A	0.102	m^2
Maximum depth	h	0.648	m
Average width/depth ratio	$b_{avg}/h = A/h^2$	0.24	(–)
Average cross-sectional area	$A_{avg} = V/L = V/9$	0.054	m^2
External load and averaged self-weight	$q = 1500 + \rho g A_{avg}$	2783	N/m
Deflection at mid-span	δ	5.0	mm

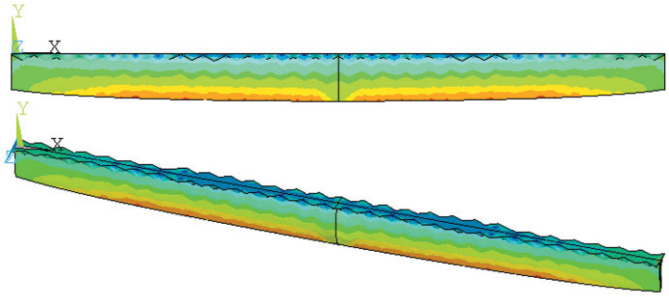

Fig. 18. Optimized result for keel mould method, test No. 33

Table 2. Results of linear analysis, test No. 82

Stiffness B25	E_c	28485	N/mm^2
Concrete volume	V	0.49	m^3
Mid-span cross-section	A	0.129	m^2
Maximum depth	h	0.675	m
Average width/depth ratio	$b_{avg}/h = A/h^2$	0.28	(–)
Average cross-sectional area	$A_{avg} = V/L = V/9$	0.054	m^2
External load and averaged self-weight	$q = 4500 + \rho g A_{avg}$	5780	N/m
Deflection at mid-span	δ	1.7	mm

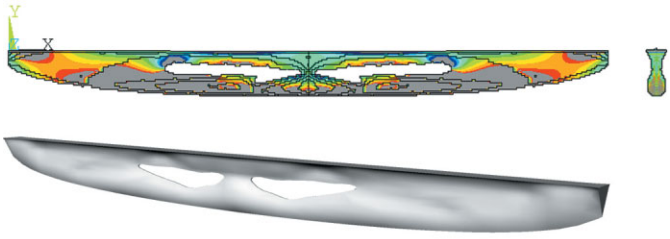

Fig. 19. Optimized result for pinch mould method, test No. 82, and rendering

where the parabolically shaped beam is defined by

$$h(x) = h_1 + h_2\left(1 - \frac{2x}{l}\right)\left(1 + \frac{2x}{l}\right) \tag{16}$$

and

$$I = \frac{1}{12} b\left(h(x)\right)^3 \tag{17}$$

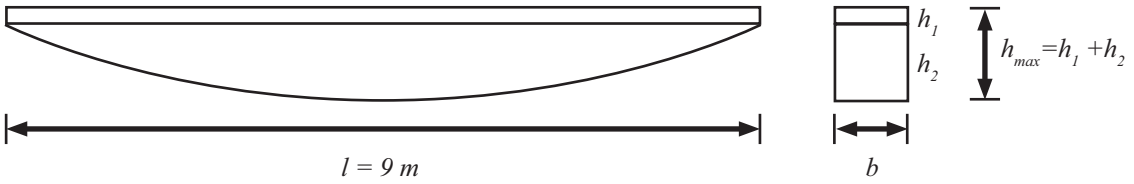

Fig. 20. Model of parabolic beam used for comparison

The displacement is assumed to be:

$$u(x) = u_1\left(1-\frac{2x}{l}\right)\left(1+\frac{2x}{l}\right) + u_2\left(1-\frac{2x}{l}\right)^2\left(1+\frac{2x}{l}\right)^2 \qquad (18)$$

This displacement function, assumed to be symmetrical, consists of two parts (*Ritz* functions): a parabola with an amplitude u_1 and a fourth-order polynomial with an amplitude u_2. Both parts fulfil the kinematic boundary conditions as required by the minimum potential energy method. It is noted that this analysis does not provide the exact solution to the beam deflection. A third part could have been added to the displacement function but the improvement to the accuracy of the calculated deflections would have been minmal.

For equilibrium, the potential energy needs to be stationary with respect to the deformation parameters. Therefore:

$$\frac{\partial E_{pot}}{\partial u_1} = 0 \text{ and } \frac{\partial E_{pot}}{\partial u_2} = 0 \qquad (19a,b)$$

The coefficients u_1 and u_2 are solved from the latter two equations. The resulting equation is too long to be shown, but gives the displacement as $\delta = \delta(q, l, E, b, h_1, h_2)$. The results of this equation for a beam with load, span and volume equal to those of the fabric-formed beam are plotted in Fig. 21.

The plot reveals an optimum where deflection is 12 % less than that of a fully parabolic ($h_1 = 0$) or rectangular beam ($h_2 = 0$), from which we can conclude that the optimum ratio h_1/h_2 is about 4/6. Another interesting conclusion is that the difference in deflection of a parabolic beam is a fraction lower – less than 1 % – than that of a rectangular beam with an equal b/h_{max} ratio. The beam corresponding to the optimum ratio 4/6 is used for comparison. The fabric-formed beam is loaded in ANSYS and the resulting deflection is compared to the rectangular and parabolic beams in Table 3. The analytical calculation of the non-prismatic beam includes only bending deformation; therefore, shear deformation and local deformations at the supports have been neglected. Due to the slenderness of the beam, the neglected deformations are expected

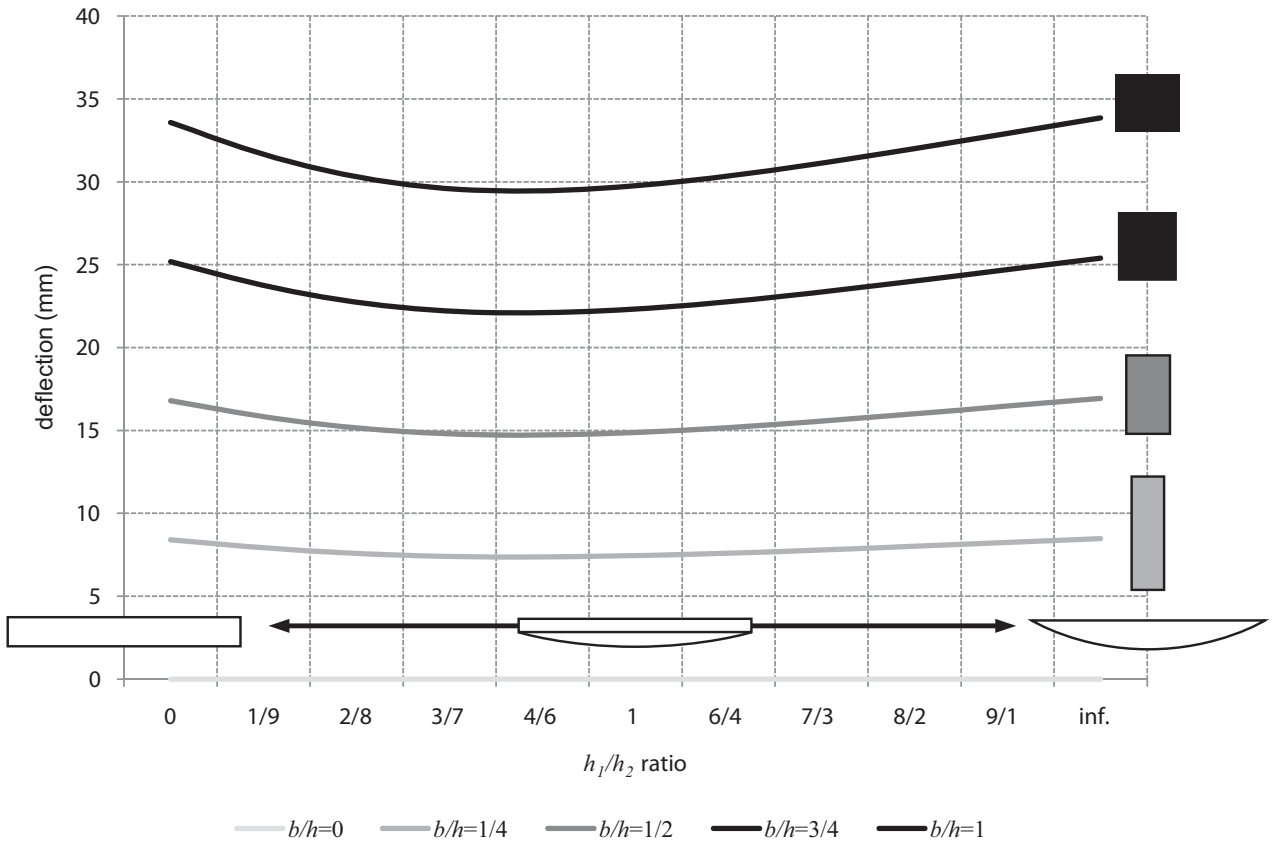

Fig. 21. Deflection of parabolic beam model depending on b/h and h_1/h_2 ratios

Table 3. Linear elastic comparison of beams of equal span and maximum depth

Beam	Volume at equal deflection	Deflection at equal volume
reference beam	100 %	100 %
parabolic beam	88 %	88 %
fabric-formed beam	42 %	42 %

to be very small. Clearly, the numerical computations do include all the deformations possible.

The reduction in volume of the fabric-formed beam is 58 %. The reason why both comparisons in Table 3 yield the same savings is that the depth and length are kept constant, and therefore the volume is dependent on one variable only, the width ($V = b \times h \times l = b \times const.$), and thus is linearly proportional to the deflection. The comparison demonstrates that gains from optimizing the longitudinal shape are smaller than those from optimizing the cross-section. From a structural point of view, the pinch mould is far more interesting to develop than the keel mould, although the latter is much simpler in terms of formwork.

It is possible to compare these results with a theoretical beam of equal cross-sectional area A that shifts all its material to the outer fibres. This beam has two flanges where the depth of the flanges h_f approaches zero and the width b_f infinity, and does not feature a web. Assuming A to be constant, $bh = b_f h_f$. The moment of inertia, using the parallel axis theorem, becomes:

$$I_d = I + Ad^2 = \frac{1}{12} b_f h_f^3 + Ad^2 \tag{20}$$

$$\lim_{h_f \to 0} I_d = 0 + Ad^2 = 2\left(\frac{1}{2} bh \cdot \left(\frac{1}{2} h\right)^2\right) = \frac{1}{4} bh^3 = 3 \cdot \frac{1}{12} bh^3 \tag{21}$$

The moment of inertia becomes $1/4 \cdot bh^3$ as opposed to $1/12 \cdot bh^3$, suggesting that for a prismatic beam in bending the theoretical lower limit for the volume reduction at equal depth and deflection will be 67 %.

10 Discussion

The emphasis of this research was on the principle of combining optimization with manufacturability and the computational framework in general as a proof of concept, leaving room for development and verification of the form-finding and analysis procedures.

The modelling of the fabric could be improved by including biaxial and non-linear material behaviour, although this is likely to be more appropriate at a later stage after the general design of the beam has been decided upon. The type of meshing can be adjusted to approximate better the fabric geometry and at the same time provide a basis for the concrete volume mesh. Also, unstructured meshing generators and refinement provided by ANSYS could not cope adequately within an automated process of random complex shapes. It is likely that if simplified cubic meshes are to be avoided, a significant challenge remains in terms of automated, flexible discretization, although commercially available mesh-less methods show promise in this context. If the relatively coarse cubic approach is retained, some error estimation would be appropriate.

The analysis of the concrete can include multiple load cases and also non-linear material behaviour to account for the reinforcement steel. As discussed, this may also improve the determination of the performance index and will have a positive effect on the overall optimization. More generally, the current framework considers neither the supporting framework for the fabric nor the requirements and design of the reinforcement, which is crucial for assessing the added value of more complex formworks such as the pinch mould. It would be worthwhile including aspects of labour, production and transportation in the model in order to compare fabric formworks fully with conventional methods.

The authors believe that the most important improvements can be made in the parametric description of complex moulds, e.g. pinch mould, and appropriate reinforcement. Related research into modern reinforcement is the key in this respect. Flexible systems such as fibre and textile reinforcement are prime candidates for combining with fabric-formed concrete as well as the notion of the fabric formwork itself functioning as reinforcement.

11 Conclusions

A computational framework has been created that combines automatic structural optimization with manufacturing constraints. It has been shown that using a general optimization algorithm allows these constraints to be introduced directly. In this respect it differs from typical examples of structural optimization that do not include manufacturability or include it only after optimization is complete, i.e. use some form of post-processing. This conceptual framework contains specific algorithms for the tasks of general optimization, fabric form-finding and concrete analysis which are independently interchangeable with similar algorithms. The constraints from any other manufacturing process could also be used in this framework, replacing the form-finding procedure.

Furthermore, the flexibility of general optimization algorithms allows non-structural objectives to be taken into account. The framework could therefore be applied to more appropriate, complex problems that include non-structural objectives, and therefore have outcomes that are relatively hard to predict based on a priori engineering judgement.

The current optimization process converges towards shapes with a higher performance, defined as the ratio of stiffness to volume. Inclusion of non-linear material behaviour for the concrete has been discussed and tested, but the computations proved to be too demanding within the scope of this project to be used for the final results. The final results show fabric-formed beams that are optimized compared with prismatic beams of rectangular cross-section as well as non-prismatic parabola-shaped beams of rectangular cross-section, significantly reducing

the amounts of concrete and steel required. The results explicitly include manufacturing information such as the amount and shape of the fabric and distribution of prestress.

12 Final remarks

The results of the optimization framework are not very surprising and could easily have been designed by an engineer as a target shape for traditional form-finding. So allowing more user interaction is suggested for the further development of design and analysis tools for fabric formworks. An architect or engineer should be able to exert more control over the geometry, preferably in a real-time, parametric environment. This train of thought is the focus of ongoing research on the computational design of fabric formworks as part of the first author's doctoral research carried out at ETH Zurich. It is believed that such interactive tools will contribute to fabric formwork achieving its full potential, thus expanding architectural vocabulary with new possibilities and ultimately transforming how people view structural concrete.

Acknowledgements

The authors would like to thank dr. ir. *Pierre Hoogenboom*, member of the first author's graduate committee, for his help with the review process of this paper and his expertise in structural mechanics.

Notation

A surface area
a acceleration
B Bézier curve
b width
b_f width of flange
Cr crossover factor
D dimension of vector
d limiting value
E_f fabric stiffness
E_k kinetic energy
E_p position energy, potential energy of external loads
E_{pot} potential energy
E'_s deformation or strain energy
EA tension stiffness
EI bending stiffness
F externally applied load
F_s scale factor
g gravity (9.81 N/kg)
h depth
h_f flange thickness
I second moment of area
K stiffness matrix
L current element length
L_0 initial element length
l span
M bending moment
m lumped nodal mass
P point
PI performance index
q distributed load
R residual force
T tension
T_0 initial tension, or pretension
t time
t_f fabric thickness
$\boldsymbol{u}$ trial vector
V volume
v velocity
$\boldsymbol{v}$ mutation vector
$\boldsymbol{x}$ base or trial vector
x position vector
δ displacement
κ curvature
ρ density

References

1. *Veenendaal, D.* et al.: History and overview of fabric formwork: using fabric for casting concrete. Structural Concrete 3, 2011, pp. 164–177.
2. *Schmitz, R. P.*: Fabric-formed concrete panel design. Proceedings of 17th Analysis & Computation Specialty Conference 2006 Structures Congress. St. Louis, 2006 (online) available at: <http://www.rpschmitz.com/linked%20media/fabric-formed%20concrete%20panel%20design-sei.pdf>
3. *Cauberg, N.* et al.: Fabric Formwork for Flexible, Architectural Concrete. Proceedings of 5th International Symposium on Fiber Reinforced Polymer Reinforcement for Concrete Structures. Sydney, 2009 (online) available at: <http://www.fabricforming.org/images/papers/FabricFormworks_fib2008.pdf>
4. *Van Mele, T., Block, P.*: A Novel Form-finding Method for Fabric Formwork for Concrete Shells. Proceedings of International Association for Shell & Spatial Structures (IASS) Symposium 2010, Shanghai, 2010.
5. *West, M.*: Flexible fabric molds for precast trusses. BFT INTERNATIONAL Betonwerk + Fertigteil-Technik 72, 10 (2006), pp. 46–52.
6. *Pedreschi, R. F.*: Studies in fabric-cast concrete. Innovation & Research 62 (2005), p. 7.
7. *Bailiss, J.*: Fabric-Formed Concrete Beams Design and Analysis. Master's thesis, University of Bath, 2006.
8. *Garbett, J.*: Bone Growth Analogy for Optimizing Flexibly Formed Concrete Beams. Master's thesis, University of Bath, 2008.
9. *Barnes, M. R.*: Form-finding and Analysis of Tension Structures by Dynamic Relaxation. International Journal of Space Structures 14, 2 (1999), pp. 89–104.
10. *Lewis. W. J.*: Tension structures: form and behaviour. Thomas Telford, London, 2003.
11. *Huang, X.* et al.: A New Algorithm for Bi-directional Evolutionary Structural Optimization. JSME International Journal Series A (2006).
12. *Price, K. V.* et al.: Differential evolution: a practical approach to global optimization. Springer, London, 2005.
13. *Lampinen, J., Zelinka, I.*: Mixed Variable Non-Linear Optimization by Differential Evolution. Proceedings of Nostradamus '99, 2nd International Prediction Conference. Zlin, 1999.
14. *Veenendaal, D.*: Evolutionary optimization of fabric-formed structural elements. Bridging the gap between computational optimization and manufacturability. Master's thesis, TU Delft, 2008 (online) available at: <http://www.fabricforming.org/images/papers/Veenendaal,%20D.,%202008.%20Evolutionary%20Optimization%20of%20Fabric%20Formed%20Structural%20Elements.pdf>

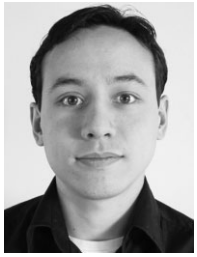

Veenendaal, Diederik, MSc, doctoral research assistant, ETH Zurich
Department of Architecture
Institute for Technology in Architecture
Wolfgang-Pauli-Strasse 15
HIL E 45.3
8093 Zurich, Switzerland
Tel.: +41 44 633 28 03
Fax: +41 44 633 10 41
veenendaal@arch.ethz.ch

Coenders, Jeroen, Ir., computation leader, Arup, researcher,
Delft University of Technology (TU Delft)
Faculty of Civil Engineering & Geosciences
BEMNext Laboratory
Stevinweg 1
Room 6.66
2628 CN Delft, Netherlands
Tel.: +31 20 3058500
Fax: +31 20 3058501
jeroen.coenders@arup.com

Vambersky, Jan, Prof. Dipl.ing. Em., Delft University of Technology (TU Delft)
Faculty of Civil Engineering & Geosciences
Design & Construction
Structural & Building Engineering
Stevinweg 1
Room S2 1.36
2628CN Delft, Netherlands
Tel.: +31 15 2783174
J.N.J.A.Vambersky@tudelft.nl

West, Mark, Prof., Associate Professor, University of Manitoba
Centre for Architectural Structures & Technology
University of Manitoba
Faculty of Architecture
Arch-2 Building
Winnipeg, MB, R3T 2N2, Canada
Tel.: (204) 474-7427
Fax: (204) 474-7533
westm@cc.umanitoba.ca